



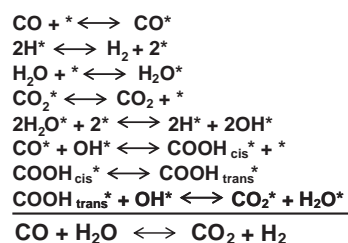
Journal of Catalysis Vol. 281, Issue 1, 2011

Contents

Microkinetic analysis and mechanism of the water gas shift reaction over copper catalysts

pp 1–11

Rostam J. Madon*, Drew Braden, Shampa Kandoi, Peter Nagel, Manos Mavrikakis, James A. Dumesic

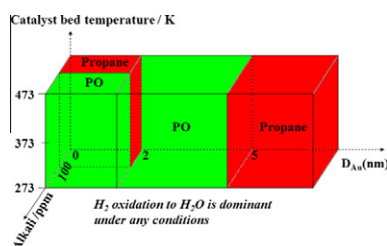


Using microkinetic modeling, we have determined the eight elementary reactions that constitute the closed catalytic cycle for the water gas shift reaction on copper catalysts. Interestingly, the most abundant surface species is bidentate formate formed via the hydrogenation of carbon dioxide which is not part of the catalytic cycle.

Switching of reactions between hydrogenation and epoxidation of propene over Au/Ti-based oxides in the presence of H₂ and O₂

pp 12–20

Caixia Qi*, Jiahui Huang, Shuangquan Bao, Huijuan Su, Tomoki Akita, Masatake Haruta*

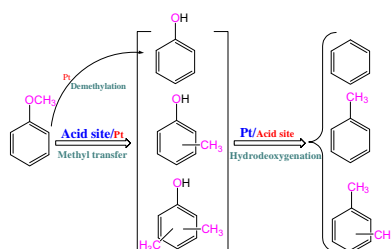


The size of Au particles and the presence of alkalis can switch hydrogenation and epoxidation of propene over Au/Ti-based oxides in a mixture with H₂ and O₂.

Bifunctional transalkylation and hydrodeoxygenation of anisole over a Pt/HBeta catalyst

pp 21–29

Xinli Zhu, Lance L. Lobban, Richard G. Mallinson, Daniel E. Resasco*

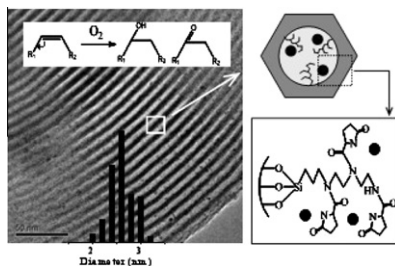


Conversion of anisole (methoxybenzene), a biomass-derived phenolic model compound, to benzene, toluene, and xylenes has been achieved over a bifunctional Pt/HBeta catalyst that catalyzes both transalkylation and hydrodeoxygenation reactions. Concerted (bifunctional) participation of acid site and metal sites in both reactions is postulated.

Superior catalytic properties in aerobic oxidation of olefins over Au nanoparticles on pyrrolidone-modified SBA-15

pp 30–39

Liang Wang, Hong Wang, Prokop Hapala, Longfeng Zhu, Limin Ren, Xiangju Meng, James P. Lewis, Feng-Shou Xiao*

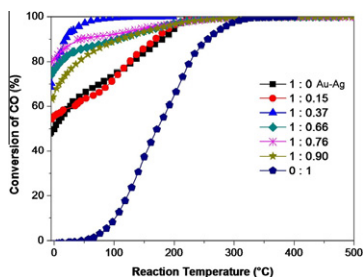


Au nanoparticles highly dispersed in the mesopores of pyrrolidone (Py)-modified SBA-15 (Au/SBA-15-Py) are efficient and stable heterogeneous catalysts for oxidations of cyclohexene and styrene by molecular oxygen at atmospheric pressure. The interaction between Au nanoparticles with Py in Au/SBA-15-Py is supported by XPS characterization, in strong agreement with density-functional theory calculations.

Bimetallic Au–Ag/TiO₂ catalyst prepared by deposition–precipitation: High activity and stability in CO oxidation

pp 40–49

Alberto Sandoval, Antonio Aguilar, Catherine Louis, Agnès Traverse, Rodolfo Zanella*



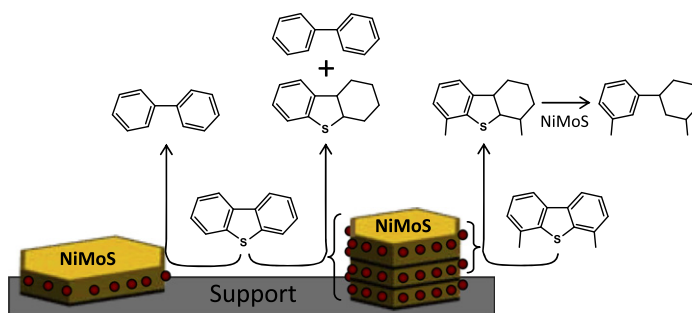
Au–Ag/TiO₂ catalysts exhibit significantly higher activity in CO oxidation at RT and a better temporal stability than monometallic gold catalysts; monometallic silver catalyst is inactive at RT. These results confirm that there is a synergistic effect between gold and silver.

Effect of the support on the high activity of the (Ni)Mo/ZrO₂–SBA-15 catalyst in the simultaneous hydrodesulfurization of DBT and 4,6-DMDBT

pp 50–62

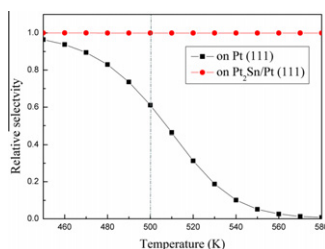
Oliver Y. Gutiérrez, Tatiana Klimova*

The hydrodesulfurization of dibenzothiophene (DBT) and 4,6-dimethyldibenzothiophene (4,6-DMDBT) on Mo- and NiMo-catalysts supported on pure oxides and ZrO₂–SBA-15 indicated that the active phase morphology was the dominant factor during the reaction. Monolayers of MoS₂ in Mo catalysts had low activity for the HDS of both DBT compounds. On NiMo catalysts, DBT reacted on monolayered and stacked NiMoS clusters, but 4,6-DMDBT was converted only on the latter.

**Theoretical study of 1,3-cyclohexadiene dehydrogenation on Pt (1 1 1), Pt₂Sn/Pt (1 1 1), and Pt₂Sn/Pt (1 1 1) surfaces**

pp 63–75

Hong-Yan Ma, Gui-Chang Wang*

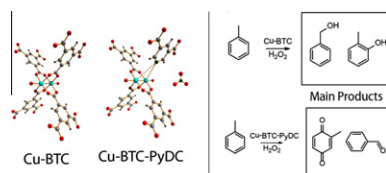


Temperature dependence of the relative selectivity of gas benzene produced by the 1,3-cyclohexadiene dehydrogenation on Pt (1 1 1) and Pt₂Sn/Pt (1 1 1) using the microkinetic modeling technique ($P_{C_6H_8} = 7.4 \times 10^{-5}$ Pa). The dashed line denotes a typical temperature at 500 K.

Synthesis, structural properties, and catalytic behavior of Cu-BTC and mixed-linker Cu-BTC-PyDC in the oxidation of benzene derivatives

pp 76–87

Stefan Marx, Wolfgang Kleist, Alfons Baiker*

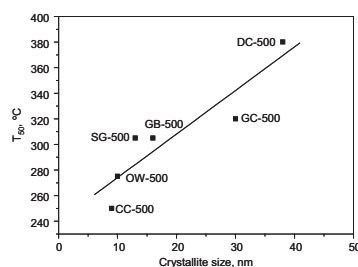


Cu-BTC was modified via partial substitution of benzene-1,3,5-tricarboxylate (BTC) linkers by pyridine-3,5-dicarboxylate (PyDC). The incorporation of PyDC into the regular lattice leads to a defined number of defect sites at the dimeric Cu units. The mixed-linker MOF showed distinct differences in the selectivity of the direct hydroxylation of benzene derivatives.

Synthesis, characterisation and catalytic performance of nanocrystalline Co₃O₄ for gas-phase chlorinated VOC abatement

pp 88–97

Beatriz de Rivas, Rubén López-Fonseca, Cristina Jiménez-González, José I. Gutiérrez-Ortiz*

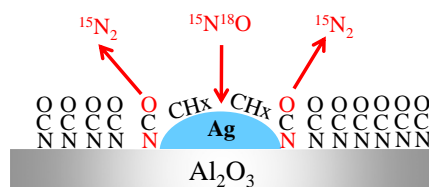


Several nanocrystalline Co₃O₄ were synthesised and investigated for their activity and selectivity during the gas-phase oxidation of 1,2-dichloroethane, a model chlorinated VOC. Activity was mainly influenced by a small crystallite size which resulted in promoted low-temperature reducibility.

The use of short time-on-stream *in situ* spectroscopic transient kinetic isotope techniques to investigate the mechanism of hydrocarbon selective catalytic reduction (HC-SCR) of NO_x at low temperatures

pp 98–105

Sarayute Chansai, Robbie Burch*, Christopher Hardacre, John Breen, Frederic Meunier

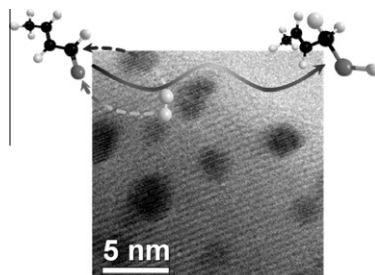


A short time-on-stream SSITKA method can discriminate between active and inactive surface species under conditions where conventional experimental methods fail.

Heteroepitaxial growth of gold on flowerlike magnetite: An efficacious and magnetically recyclable catalyst for chemoselective hydrogenation of crotonaldehyde to crotyl alcohol

pp 106–118

Yuan Zhu, Li Tian, Zheng Jiang, Yan Pei*, Songhai Xie, Minghua Qiao*, Kangnian Fan

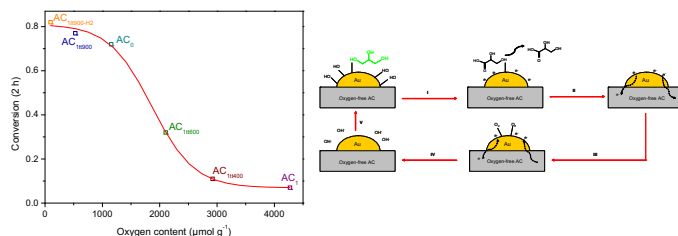


Gold supported on flowerlike magnetite shows excellent catalytic performance in liquid phase hydrogenation of crotonaldehyde to crotyl alcohol. A perimeter interface mechanism is established to account for its superior selectivity.

Influence of activated carbon surface chemistry on the activity of Au/AC catalysts in glycerol oxidation

pp 119–127

Elodie G. Rodrigues, Manuel F.R. Pereira, Xiaowei Chen, Juan J. Delgado, José J.M. Órfão*

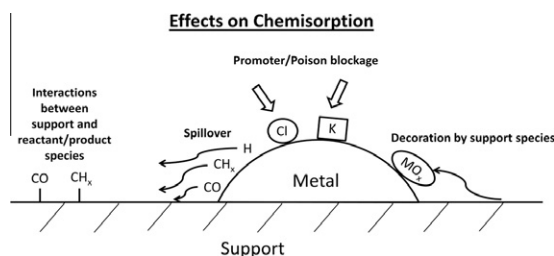


The oxygen content of activated carbon surface plays a key role on the activity of Au/AC catalysts for the oxidation of glycerol. Oxygen-free supports promote electron mobility, which enhances the catalytic performance.

Comparison of chemisorption close to ambient vs. under reaction conditions for Group VIII metal catalysts

pp 128–136

Yu-Tung Tsai, James G. Goodwin Jr.*

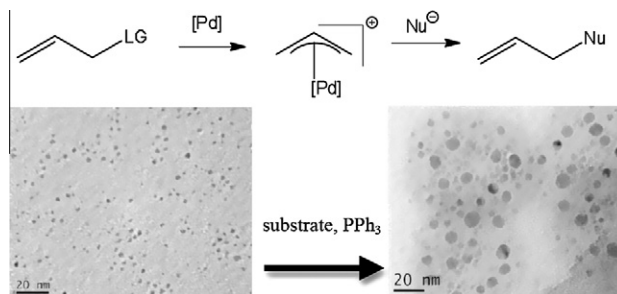


Static chemisorption measured at low temperature may overestimate metal dispersion as a result of spillover or underestimate it due to slow kinetics of adsorption, strong metal-support effects (SMSI), and/or the presence of promoters or poisons.

Size- and shape-controlled palladium nanoparticles in a fluorometric Tsuji–Trost reaction

pp 137–146

Yuwei Yang, Larry D. Unsworth, Natalia Semagina*

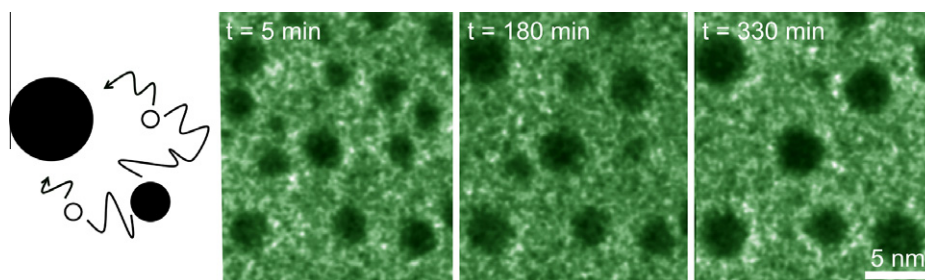


Pd nanoparticles catalyze Tsuji–Trost reaction for Pd fluorometric detection in the presence of PPh₃ via atomic dissolution.

Ostwald ripening in a Pt/SiO₂ model catalyst studied by *in situ* TEM

pp 147–155

Søren Bredmose Simonsen, Ib Chorkendorff, Søren Dahl, Magnus Skoglundh, Jens Sehested, Stig Helveg*

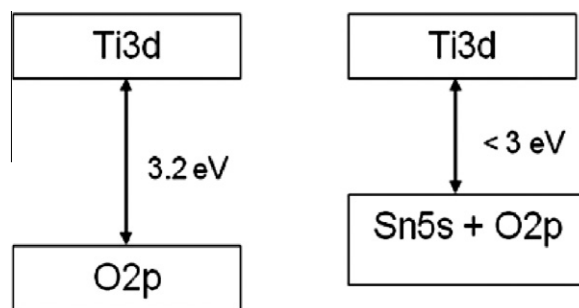


Sintering of Pt nanoparticles on SiO₂ support was studied by *in situ* transmission electron microscopy (TEM) under oxidizing conditions. Time-lapsed TEM images reveal that the sintering is governed by Ostwald ripening and is better described by kinetic models, including local correlations between the Pt particles.

Photocatalytic degradation of organic molecules on mesoporous visible-light-active Sn(II)-doped titania

pp 156–168

Venkata Bharat Ram Boppana, Raul F. Lobo*

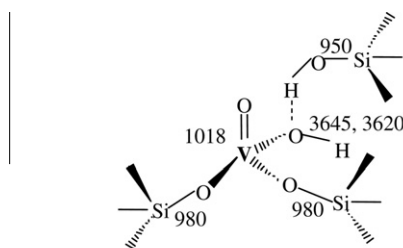


Visible-light-active valence band-hybridized Sn(II)-TiO₂ materials were synthesized possessing unique electronic properties and photocatalytic activities dependent on the hydrothermal synthesis conditions.

Methanol oxidation on VSiBEA zeolites: Influence of V content on the catalytic properties

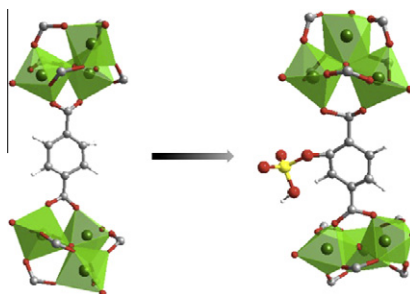
pp 169–176

Maciej Trejda*, Maria Ziolek, Yannick Millot, Karolina Chalupka, Michel Che, Stanislaw Dzwigaj*

**Pseudo-tetrahedral hydroxylated (SiO)₂(HO)V=O species****Sulfation of metal–organic frameworks: Opportunities for acid catalysis and proton conductivity**

pp 177–187

Maarten G. Goesten, Jana Juan-Alcañiz, Enrique V. Ramos-Fernandez, K.B. Sai Sankar Gupta, Eli Stavitski, Herman van Bekkum, Jorge Gascon*, Freek Kapteijn

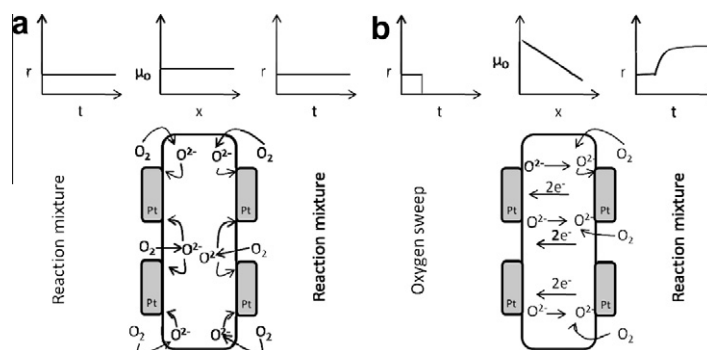


A new post-functionalization method to incorporate sulfoxyl acid moieties in different MOFs has been developed. The sulfated frameworks show outstanding catalytic activity in esterification and a high proton conductivity.

Controlled spillover in a single catalyst pellet: Rate modification, mechanism and relationship with electrochemical promotion

pp 188–197

Danai Poulidi*, Maria Elena Rivas, Ian S. Metcalfe



The effect of spillover processes on the activity of a catalyst system consisting of a mixed oxygen ion and electron conducting support (La_{0.6} Sr_{0.4} Co_{0.2} Fe_{0.8} O_{3-δ}) and a metal catalyst (Pt) were investigated. Driving forces for promoter migration were controlled through the manipulation of the oxygen chemical potential difference across the catalyst which was in the form of a pellet membrane. It was found that there is a complex relationship between the rate modification through spillover, the driving forces for spillover and the geometrical arrangement of the catalyst on the support (i.e. catalyst dispersion).